

# (Guanidine)copper Complex-Catalyzed Enantioselective Dynamic Kinetic Allylic Alkynylation Under Biphasic Condition

Xi-Yang Cui<sup>1</sup>, Yicen Ge<sup>1</sup>, Siu Min Tan<sup>2</sup>, Huan Jiang<sup>1</sup>, Davin Tan<sup>1,2</sup>, Yunpeng Lu<sup>1</sup>, Richmond Lee<sup>2\*</sup>, Choon-Hong Tan<sup>1\*</sup>

<sup>1</sup>Division of Chemistry and Biological Chemistry, Nanyang Technological University, 21 Nanyang Link, Singapore 637371

<sup>2</sup>Singapore University of Technology and Design, 8 Somapah Road, Singapore 487372

**ABSTRACT:** Highly enantioselective allylic alkylation of racemic bromides under biphasic condition is furnished in this report. This approach employs functionalized terminal alkynes as pro-nucleophiles and provides 6- and 7-membered cyclic 1,4-enynes with high yields and excellent enantioselectivities (up to 96% ee) under mild conditions. Enantio-retentive derivatizations highlight the synthetic utility of this transformation. Cold-spray ionization mass spectrometry (CSI-MS) and X-ray crystallography were used to identify some catalytic intermediates, which include guanidinium cuprate ion pairs and a copper-alkynide complex. A linear correlation between the enantiopurity of the catalyst and reaction product indicates the presence of a copper complex bearing a single guanidine ligand at the enantio-determining step. Further experimental and computational studies supported that the alkylation of allylic bromide underwent an *anti*-S<sub>N</sub>2' pathway catalyzed by nucleophilic cuprate species. Moreover, metal-assisted racemization of allylic bromide allowed the reaction to proceed in a dynamic kinetic fashion to afford the major enantiomer in high yield.

## INTRODUCTION

Enantioselective allylic substitutions are powerful synthetic methods to strategically install C-C bonds.<sup>1</sup> There are two main approaches for catalytic enantioselective allylic substitutions: 1) a new stereogenic center is generated from a prochiral substrate *via* S<sub>N</sub>2' pathway or 2) resolution from racemic chiral starting materials (maximum yield of 50%). The development of dynamic kinetic processes broke the yield limit for the resolution approach and the use of stabilized nucleophiles (Nuc-H pK<sub>a</sub> <25)<sup>2</sup> in Pd-catalyzed dynamic kinetic asymmetric transformation is particularly successful.<sup>3</sup>

On the other hand, low-cost copper shows great compatibility with non-stabilized nucleophiles (Nuc-H pK<sub>a</sub> >25).<sup>4,5</sup> Unlike reactions with stabilized nucleophiles, which add in an outer-sphere manner, the control of non-stabilized nucleophiles in allylic substitutions requires the metal catalyst to modulate the reactivity of both the allylic substrate and nucleophile.<sup>4c</sup> This is further complicated by the fact that during dynamic kinetic reactions, the enantiomers of the starting material may have different rates of addition, isomerization and elimination when interacting with the chiral metal complex.<sup>5h</sup> Due to the high pK<sub>a</sub> values of non-stabilized nucleophiles, the pro-nucleophiles used for such reactions are typically organometallic reagents, which are readily transmetallated to the metal catalyst. The functional group tolerance is generally low or moderate at room temperature towards these active organometallic reagents.<sup>4</sup> Therefore, it is not surprising that it is only recently that Cu-catalyzed dynamic kinetic enantioselective allylic substitutions with non-stabilized nucleophiles, mainly to construct C<sub>sp3</sub>-C<sub>sp3</sub> bonds, have been achieved through the efforts of Alexakis and Fletcher.<sup>5</sup>

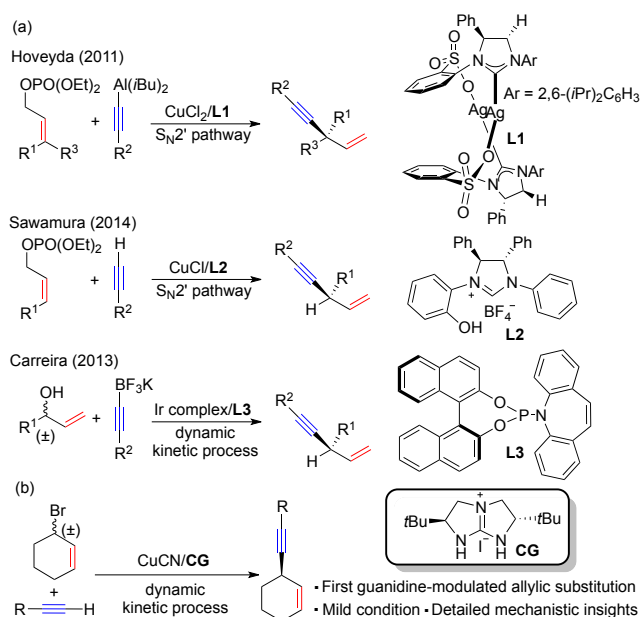


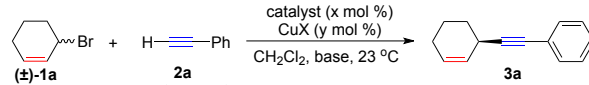
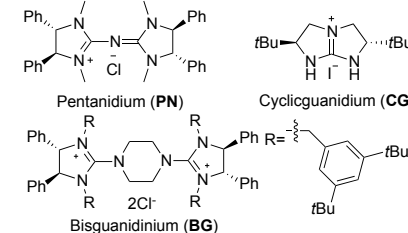
**Figure 1.** C<sub>sp3</sub>-C<sub>sp</sub> bond construction *via* enantioselective allylic substitution. a) Successful examples using alkynes or equivalents in enantioselective allylic substitutions. b) Guanidine(copper) complex-catalyzed dynamic kinetic enantioselective allylic alkylation (this work).

The formation of C<sub>sp3</sub>-C<sub>sp</sub> bond through asymmetric allylic alkylation is challenging but rewarding, as it leads to highly functionalized 1,4-enynes (skipped enynes)<sup>6</sup> and to date, there are only three successful examples (Figure 1a).<sup>7</sup> Using a mix of Cu/NHC-Ag catalyst system, Hoveyda reported the first example of allylic alkylation employing organoaluminium reagents.<sup>7a</sup> The reaction proceeded *via* the S<sub>N</sub>2' pathway with a variety of allylic phosphates. A significant improvement was subsequently reported by

Sawamura who demonstrated that terminal alkyne pronucleophiles can be activated directly using a Cu-carbene catalyst and high enantioselectivities were achieved with trisopropylsilylacetylenes.<sup>7b</sup> In both examples, chiral *N*-heterocyclic carbene ligands played key roles to modulate reactivity and selectivity. The only example of allylic alkylation using racemic chiral substrates, through a dynamic kinetic process, is the direct displacement of linear allylic alcohols with alkynyltrifluoroborates, utilizing an Ir-phosphoramidite catalyst.<sup>7c</sup> The enantioselective formation of C<sub>sp3</sub>-C<sub>sp</sub> bond through dynamic kinetic allylic alkylation with Cu-catalyst is still unexplored until this work.

Guanidine is known to coordinate with various metals in different modes.<sup>8</sup> However, successful examples using chiral guanidine as ligands in metal-catalyzed asymmetric reactions are scarce and are only emerging recently.<sup>9</sup> Reported reactions are limited to X-H (X = N or C) insertion with carbene precursor,<sup>9a,9b</sup> nucleophilic addition<sup>9c</sup> and Ullman reaction<sup>9d,9e</sup>. In the past decade, our group has developed guanidine, conjugate-guanidinium (pentanidium) and bis-guanidinium as organocatalyst, phase transfer catalyst and ion-pairing catalyst respectively.<sup>10</sup> Herein, we present our efforts to expand the chemistry of guanidine to include the use of (guanidine)copper complexes to catalyze allylic alkylation of racemic bromides (Figure 1b).

**Table 1. Chiral Cation/Cuprate-Catalyzed Enantioselective Alkylation<sup>a</sup>**

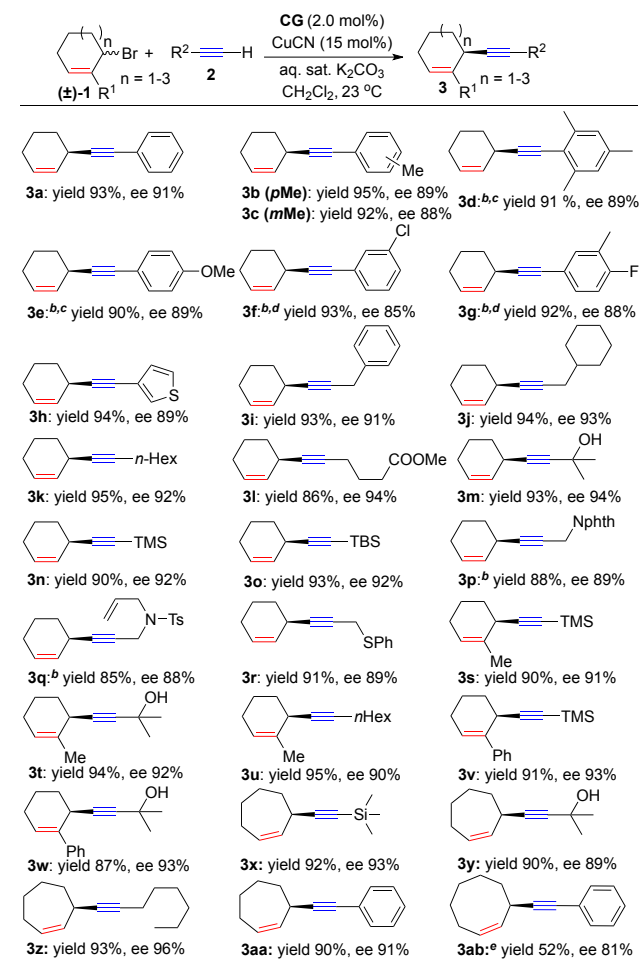
entry	catalyst/ x mol%	CuX/ y mol%	base	yield (%) <sup>b</sup>	ee (%) <sup>c</sup>
1	PN (2)	CuCl (20)	50 wt% NaOH	92	0
2	BG (2)	CuCl (20)	50 wt% NaOH	90	17
3	CG (2)	CuCl (20)	50 wt% NaOH	90	25
4	CG (2)	CuCl (20)	aq. sat. K <sub>2</sub> CO <sub>3</sub>	76	79
5	CG (2)	CuBr (20)	aq. sat. K <sub>2</sub> CO <sub>3</sub>	75	76
6	CG (2)	CuI (20)	aq. sat. K <sub>2</sub> CO <sub>3</sub>	72	60
7	CG (2)	CuCN (20)	aq. sat. K <sub>2</sub> CO <sub>3</sub>	80	89
8 <sup>d</sup>	CG (2)	CuCN (15)	aq. sat. K <sub>2</sub> CO <sub>3</sub>	85	91

<sup>a</sup>Reaction was carried out with **1a** (0.05 mmol) and **2a** (0.05 mmol) in CH<sub>2</sub>Cl<sub>2</sub> (1 mL) and base (0.5 mL) for 12 h under N<sub>2</sub> atmosphere. <sup>b</sup>GC yield, 1,1'-biphenyl used as an internal standard. <sup>c</sup>Determined by GC-MS analysis with a chiral column. <sup>d</sup>1.6 equiv. allylic bromide was used, ee of the recovered **1a** was 0%.

## RESULTS AND DISCUSSION

**Enantioselective Alkylation of Cyclic Allylic Bromides.** We were initially motivated by examples in the literature demonstrating that Cu-catalyzed allylic substitutions can proceed at room temperature under biphasic conditions.<sup>11</sup> Using the allylic alkylation reaction between bromocyclohexene (**1a**) and phenylacetylene (**2a**) as the model reaction, we investigated several chiral cations developed in our laboratory under phase transfer conditions (Table 1). In the presence of copper(I) chloride, pentanidium (**PN**)<sup>12</sup> showed good reactivity but no enantioselective induction was detected (Table 1, entry 1). When 2 mol% of bisguanidinium (**BG**) was used, skipped enyne **3a** was obtained in good yields with moderate enantioselectivity (entry 2). Cyclic-guanidinium (**CG**),<sup>13</sup> previously prepared as a Brønsted base or phase transfer catalyst in our laboratory, gave the highest level of enantioselectivity after initial investigations (entry 3). It was found that a weaker base improved the enantioselectivity by suppressing background reaction and aqueous saturated K<sub>2</sub>CO<sub>3</sub> was the most ideal (entries 4-8). It was also found that CuCN was the most suitable copper salt (entries 4-8). Solvent studies, leaving group studies and detailed optimization data are provided in the supporting information (see SI, Table S1-S2).

**Scheme 1. Enantioselective Alkylation of Cyclic Allylic Bromides.<sup>a</sup>**

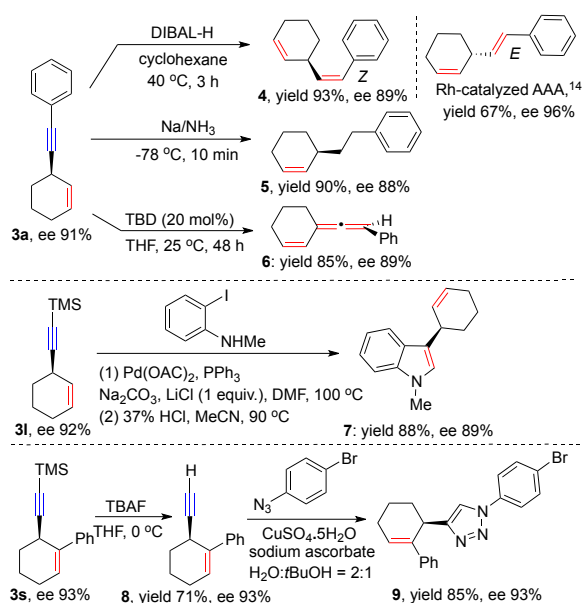


<sup>a</sup>Reactions were carried out with alkynes (0.4 mmol) and allylic bromides (0.64 mmol) in CH<sub>2</sub>Cl<sub>2</sub> (7.0 mL) and sat. K<sub>2</sub>CO<sub>3</sub> (3.5 mL) for 24 h under N<sub>2</sub> atmosphere; yields refer to isolated yields

and ee values were determined using chiral GC or HPLC. <sup>b</sup>4 mol % of guanidinium salt and 10 mol % of CuCN were used. <sup>c</sup>Reaction time is 36 h. <sup>d</sup>Reaction time is 16 h. <sup>e</sup> Reaction time is 48 h.

With the optimized reaction conditions in hand, the substrate scope of the reaction was examined (Scheme 1). Various aryl-substituted terminal alkynes were useful with this methodology (Scheme 1, **3a-h**) including aromatic heterocycles such as 3-thienyl-substituted alkyne (**3h**). Benzyl-, cyclohexyl- and *n*hexyl-substituted terminal alkynes also gave good yields and high ee values (**3i-3k**). Alkynes containing ester (**3l**), tertiary hydroxyl (**3m**), silyl (**3n, 3o**), imide (**3p**, NPhth = phthalimido), sulfonamide (**3q**) and thioether (**3r**) are generally well tolerated and provides good yields and ee values of the skipped enynes.  $\beta$ -Substituted cyclic allylbromides show no negative effect on yields and enantioselectivities (**3s-3w**). 3-Bromocyclopentenes were unstable under the reaction condition; thus, no desired product was observed. On the other hand, seven-membered allylbromides were suitable and provided good results for the asymmetric allylic alkylation (**3x-3aa**). The reactivity for eight-membered cyclic allylic bromides was low; although a good level of enantioselectivity was obtained (**3ab**). We were able to scale up the reaction yielding **3a** (1.02 g) in gram quantity (see SI, Page S13).

## Scheme 2. Enantio-retentive Derivatizations of Enantiopure Cyclic 1,4-Enynes.



Enantiopure cyclic 1,4-enynes are versatile building blocks in organic synthesis (Scheme 2) and we demonstrate it through a series of reactions that retain their enantiopurity. When treated with diisobutylaluminum hydride (DIBAL-H), skipped enyne **3a** was smoothly converted into *Z,Z*-1,4-diene **4** in excellent yields. The other geometric isomer, *Z,E*-1,4-diene, can be directly prepared from Rh-catalyzed asymmetric allylic substitution.<sup>14</sup> When we reduced skipped enyne **3a** in Na/NH<sub>3</sub> at -78 °C, the alkyne was directly reduced to the alkane with the benzene unscathed, providing alkene **5** with retention of chirality. The absolute configuration of 1,4-enynes **3** were determined

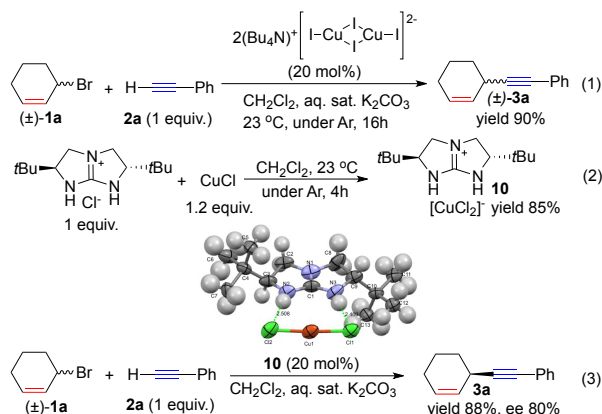
by comparing with literature value of optical rotation of alkene **5**.<sup>5e</sup> Enantiospecific base-catalyzed 1,3-proton isomerization reaction was conducted using triazabicyclodecene (TBD) and provided allene **6**.<sup>15</sup> The stability of the skipped enyne's chirality encouraged us to be adventurous and we successfully used **3l** in Larock annulation, obtaining indole **7** after removal of the silyl group.<sup>16</sup> After deprotection of the silyl group in skipped enyne **3s**, alkyne **8** underwent a Cu-catalyzed alkyne-azide cycloaddition (CuAAC) smoothly to afford triazole **9**.<sup>17</sup>

## MECHANISTIC STUDIES

### Identification of Reaction Intermediates and Mechanistic Studies.

It was proposed by Alper that quaternary ammonium alkynylcuprate complex was a key intermediate in copper-catalyzed allylation reaction of alkynes.<sup>11b</sup> We found that commercially available ammonium cuprate ion-pair (Sigma-Aldrich, Inc.),<sup>18</sup> which is soluble in CH<sub>2</sub>Cl<sub>2</sub>, catalyzed alkynylation successfully under biphasic conditions (Scheme 3, eqn. 1). As *tetra*-butyl ammonium (Bu<sub>4</sub>N<sup>+</sup>) is unlikely to act as a ligand to copper, it is most reasonable to propose that *tetra*-butyl ammonium alkynylcuprate<sup>19</sup> ion-pair is the active catalyst in this reaction. During our initial investigations, we found that a variety of chiral cations including cyclic-guanidinium (**CG**) can 'carry' copper salts into the non-polar solvents (Table 1). Indeed, guanidinium cuprate **10** was isolated as yellow solid when CuCl was mixed with CG+Cl<sup>-</sup> in CH<sub>2</sub>Cl<sub>2</sub> and a single crystal suitable X-ray diffraction was grown by vapor diffusion of Et<sub>2</sub>O into a CH<sub>2</sub>Cl<sub>2</sub> solution (Scheme 3, eqn. 2). The dichlorocuprate anion is shown to form dual hydrogen bonds with the cyclic-guanidinium cation. When this ion pair **10** was added to the reaction, asymmetric alkylation proceeded with good reactivity and stereocontrol (Scheme 3, eqn. 3), indicating that this ion pair is an intermediate or catalyst precursor in (guanidine)copper-catalyzed enantioselective allylic alkylation.

### Scheme 3. Identification of Guanidinium Cuprate Ion Pair as Catalyst Precursor.



Using cold-spray ionization mass spectrometry (CSI-MS),<sup>20</sup> we observed a new species at *m/z* = 509.354 (positive mode) when adding **10** into the basic condition and it was assigned to be dimeric (guanidine)copper complex **11** (Scheme 4a). The anion of this complex should be [CuCl<sub>2</sub>]<sup>-</sup>, similar to a complex reported by Coles.<sup>8b</sup> We found that (guanidine)copper complex **11** can also be observed when

CuCl is treated with the corresponding cyclic-guanidine (free base) directly. We further postulate the presence of a neutral monomeric (guanidine)copper complex **12** through ligand exchange with **11**.<sup>8a</sup> After the addition of alkyne **2a** to (guanidine)copper complex **10**, a cationic peak corresponding to copper alkynide intermediate **13** (Scheme 4b) was observed at  $m/z = 673.308$  (positive mode). We also postulate that intermediate **13** is the source of active, monomeric copper alkynide **14** since copper alkynides are liable to polymerization<sup>21</sup> and we found that polymeric copper alkynides *poly-15* is an insoluble solid side product in our reaction (<5%). Further experiments showed that polymeric copper alkynide *poly-15* goes through a non-catalytic pathway very slowly, which is consistent with the fact that lower enantioselectivities were observed when it is used directly for this reaction (Scheme 4c). The presence of a monomeric (guanidine)copper complex **14** was further supported by the absence of non-linear effect (NLE).<sup>22</sup> A linear relationship was observed between ee of the catalyst and ee of the product **3a** in (guanidine)copper-catalyzed allylic alkynylation (Figure 2). The result indicated that the enantio-determining copper complex is likely to bear only a single guanidine ligand.

#### Scheme 4. Identification of Guanidine(copper) Complexes as Reaction Intermediates.

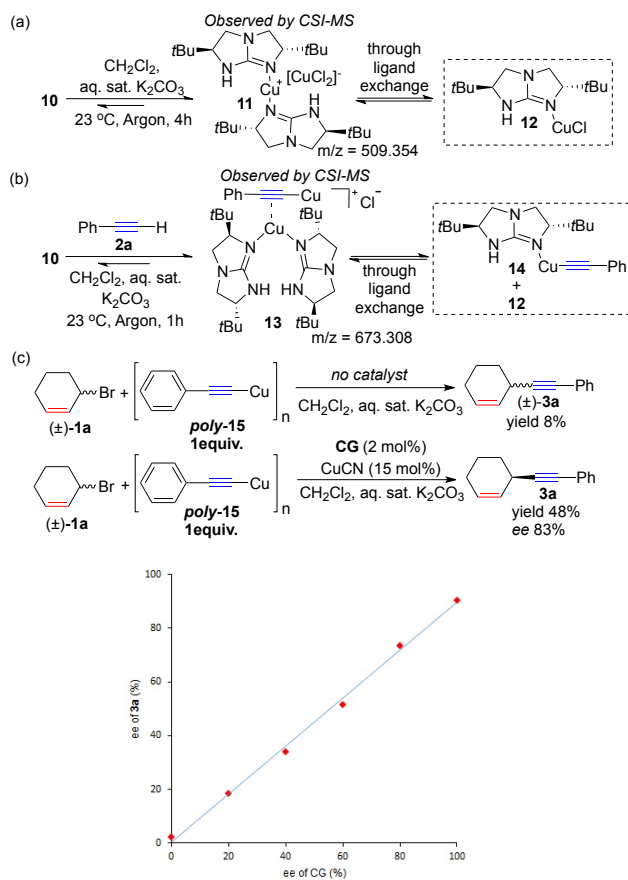
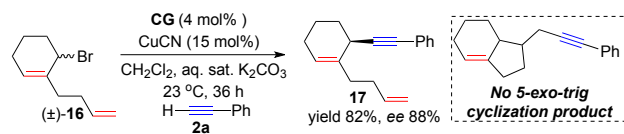


**Figure 2. A linear relationship between ee of catalyst and ee of product **3a**.**

When 2,2,6,6-tetramethylpiperidinyloxy (TEMPO) was used as a radical scavenger, the reaction was unaffected.

Recently, copper-catalyzed coupling reactions with racemic substrates through enantioconvergent radical pathways were reported by Fu.<sup>23</sup> In order to study the possibility of an inner-sphere radical intermediate, we tested radical-probe **16** and we did not observe any *5-exo-trig* cyclization product. Only skipped enynes **17** was obtained in 82% yield and 88% ee and this result demonstrated that the radical processes are unlikely involved in (guanidine)copper-catalyzed allylic alkynylation (Scheme 5).

#### Scheme 5. Radical-clock Experiment.



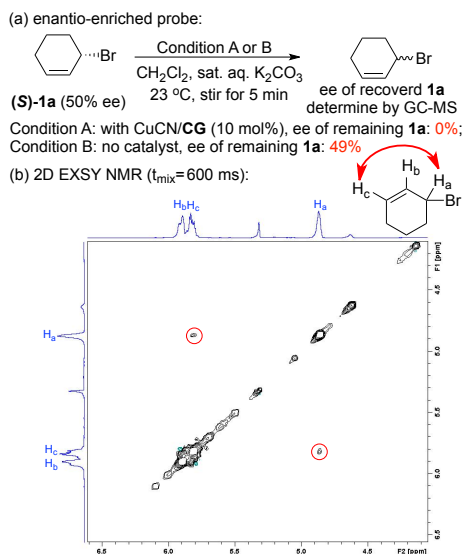
There are several proposed mechanistic pathways for Cu/phosphine-catalyzed dynamic kinetic alkylation with cyclic racemic substrates (see SI, Figure S5). The initial mechanism proposed by Alexakis for Cu-catalyzed allylic alkylation of primary Grignard reagents is similar as Pd-catalyzed DYKAT, proceeding through a prochiral or pseudo-*meso*- $\pi$ -allyl-Cu intermediate.<sup>5a</sup> However, based on further experimental studies and density functional theory (DFT) calculations,<sup>5d</sup> it was suggested that the fast reductive elimination step removed the possibility of DYKAT (through  $\eta^1$ - $\eta^3$ - $\eta^1$ -allyl equilibrations). The mechanism was then modified to a direct enantio-convergent transformation (DET),<sup>24</sup> where the enantiomers proceed through two different oxidative addition pathways (at different rates) to the same  $\sigma$ - $\pi$ -enylcopper(III) intermediate before the reductive elimination step.

For Cu-catalyzed allylic alkylation with alkylzirconium reagents, it was proposed by Fletcher, after 2D EXSY NMR (Exchange Spectroscopy) studies, that the allylic halides racemize by forming allylic iodide through metal-assisted *syn*- $\text{S}_{\text{N}}2'$  reaction and one of the enantiomer is preferred by the chiral copper complex to form the major product.<sup>5e</sup> This dynamic kinetic resolution (DKR) is catalyzed by complex oligomeric catalysts, which evolved during the reaction to become more active and more enantioselective. Only copper complexes with phosphine ligands, not NHC ligands, can trigger the *syn*- $\text{S}_{\text{N}}2'$  reaction with the iodine source.<sup>5h</sup> We performed 2D EXSY NMR to investigate the possibility of ligand-dependent *syn*- $\text{S}_{\text{N}}2'$  reaction between allylic bromide **1a** and allylic cyanide. We found that the reaction is not reversible (see SI, Figure S6a & S6b). During the initial reaction optimization, we had added the corresponding guanidine (free base) of CG into the reaction (absence of iodide) and observed the same reaction profile, which ruled out that trace amount of allylic iodide act as an intermediate in the racemization.

On the other hand, we found that at any time of our experiment, allylic bromide **1a** always remains as a racemate (chiral GC-MS analysis, see SI, Figure S6c), which encouraged us to propose that allylic bromide **1a** rapidly racemizes by isomerization. The cyclic allylic halides were reported to racemize easily through *syn*- $\text{S}_{\text{N}}2'$  pathway catalyzed by acid<sup>25a</sup>, anion<sup>25b,c</sup> and metal complex.<sup>5h</sup> We also observed the fast racemization of allylic bromide, when using enantio-enriched (*S*)-**1a** (ee 50%)<sup>26</sup> was utilized in

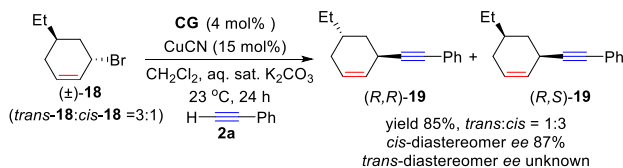
presence of our catalytic system (Scheme 6a, also see SI, Figure S6d). Using 2D EXSY NMR, we observed the chemical exchange between  $H_a(\text{Br})$  and  $H_c(\text{Br})$  of **1a** in the presence of (guanidine)copper complex (Scheme 6b, also see SI, Figure S6e).<sup>5e</sup> These results indicated that the presence of (guanidine)copper complex significantly accelerates the racemization of allylic bromides, probably through *syn*- $S_N2'$  isomerization, which is essential for a successful dynamic kinetic resolution.

### Scheme 6. Observation of Racemization of **1a**.



Stabilized nucleophiles in Pd-catalyzed DYKATs are known to antarafacially attack on the carbon of a preformed  $\pi$ -allyl-Pd intermediate resulting in the double inversion mechanism.<sup>27</sup> Whereas, non-stabilized nucleophiles tend to attach themselves to the metal center firstly through metalation; this is usually followed by an antarafacial process and thus led to *anti*-diastereospecific products through the single inversion mechanism.<sup>28,29</sup> To the best of our knowledge, the propensity of alkyne to undergo an inversion pathway has not been studied. We tested an ethyl-substituted stereo-probe **18** (*dr* 3:1) under the reaction condition and single inversional products **19** (*dr* 1:3) were obtained with 85% yield. *cis*-**19** was determined to be 87% ee while the ee of *trans*-**19** was unknown due to separation problems (Scheme 7). Considering that alkyne has a high affinity to copper,<sup>21a</sup> this result indicates that it is likely that this reaction occurs in an antarafacial manner.

### Scheme 7. Mechanistic Investigation of Alkynide Substitution Using a Stereo-probe



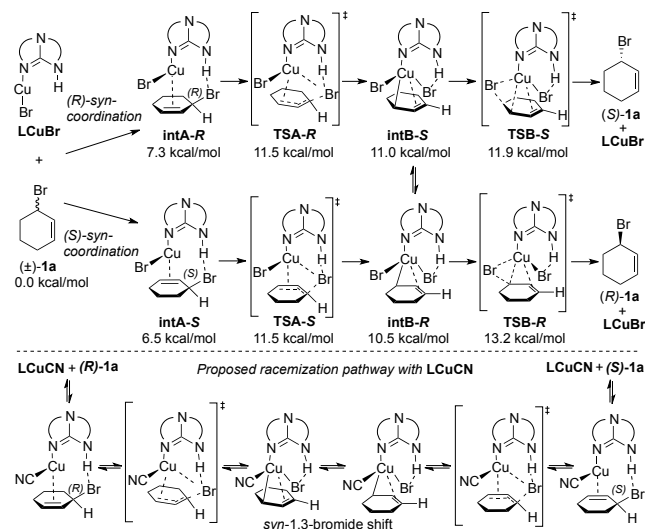
## THEORETICAL MODELING STUDIES

Mechanistic studies above revealed that racemization is a suprafacial *syn*- $S_N2'$  process (Scheme 6) and addition of alkyne occurs antarafacially with single inversion (Scheme 7). In order to construct a feasible theoretical

model, we propose LCuBr as the catalytic species responsible for the racemization process. LCuBr has a vacant coordination site which **1a** can bind and this lead to  $\text{C}_{\text{allylic}}\text{-Br}$  bond dissociation aided by intramolecular N-H $\cdots$ Br hydrogen bonding (Scheme 8, top). Our DFT calculations supported the hypothesis that (*R*)-**1a** and (*S*)-**1a** could racemize rapidly with LCuBr through a hydrogen-bonding promoted *syn*-oxidative addition and reductive elimination<sup>32</sup> (Scheme 8, top).

We would also expect LCuCN to be able to perform racemization through *syn*-coordination to **1a** and Br abstraction to form the oxidative addition intermediate. It is then rationally feasible to consider the interconversion between the two enantiomers involving a *syn*-1,3-bromide shift within the allylic group, aided by hydrogen bonding with the catalyst (Scheme 8, bottom).

### Scheme 8. Mechanistic Free Energy Profiles for the Racemization of Allylic Bromide **1a**.



The LCuR catalytic species like **14** was used to model the alkylation process *via* several pathways, namely, the concerted *anti*- $S_N2$  (see SI, Figure S7b), the concerted *anti*- $S_N2'$  (see SI, Figure S7b) and *syn*- $S_N2'$  oxidative addition/reductive elimination (Figure 3). Of these pathways, the *syn*- $S_N2'$  oxidative addition/reductive elimination pathway was found to be most energetically favorable. For this step-wise pathway, DFT calculations revealed that the rate-determining step is the reductive elimination/alkynylation process, which has free energy barriers ( $\Delta G^{\ddagger}_{\text{DCM}}$ ) of +17.7 kcal/mol leading to (*S*)-**3a** (TSD-*S*) and +16.8 kcal/mol leading to (*R*)-**3a** (TSD-*R*). However, as this pathway does not lead to stereo-inversion of the product and is inconsistent with our experimental mechanistic studies, we sought to consider an alternative active catalytic species.

Thus, on the basis of the mechanistic and the NLE experiments (Figure 2), we considered alternative mechanisms with more nucleophilic<sup>19</sup> anionic (guanidine)copper complexes  $[\text{LCu}(\text{R})\text{X}]^-$  (R = alkynides; X = Br or CN) as the active catalytic species (Figure 4), similar to the ones reported by Sawamura<sup>6b,7b,30c</sup>. Upon antarafacial (*anti*)-coordination between bromocyclohexene with the catalysts, our calculations showed that either a  $S_N2$  or  $S_N2'$  type

alkynylation could proceed,<sup>31</sup> to furnish the *R*- and *S*-product.

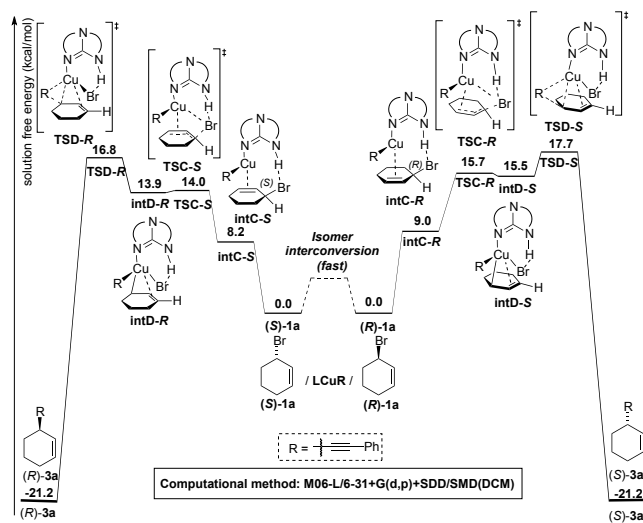


**Figure 3. Mechanistic Free Energy Profiles for the *syn*- $S_N2'$  Oxidative Addition/Reductive Elimination Pathway with  $LCuR$ .** Relative solution free energies, in kcal/mol, are shown ( $R$  = phenyl alkynide,  $L$  = chiral guanidine ligand).

The calculated free energies of the transition state structures (TS) for  $S_N2$  pathway are generally higher than  $S_N2'$  pathway by 1.2 to 4.9 kcal/mol. Therefore, only  $S_N2'$  TS will be considered in the further discussion (See SI, Figure S8a).

For  $[LCu(R)Br]^-$ , DFT calculations first optimized a slightly exergonic  $\pi$ -complex  $intE-R$  ( $\Delta G_{DCM} = -0.2$  kcal/mol) and endergonic complex  $intE-S$  ( $\Delta G_{DCM} = +2.0$  kcal/mol) (Figure 4). From  $intE-R$ ,  $S_N2'$  ( $\Delta G_{DCM}^{\ddagger}(TSE-R) = +12.7$  kcal/mol relative to  $intE-R$ ) proceeds with reasonable energy barrier forming the C-C bond between the alkynyl group directly generating  $(R)$ -3a product. Similarly, from  $intE-S$ ,  $S_N2'$  ( $\Delta G_{DCM}^{\ddagger}(TSE-S) = +16.4$  kcal/mol relative to  $intE-R$ ) pathway generates the  $(S)$ -3a product.

Overall, forming  $(R)$ -3a via  $TSE-R$  would be the most kinetically competitive pathway. This translates to a barrier difference of  $\Delta\Delta G_{DCM}^{\ddagger} = 3.7$  kcal/mol. For  $[LCu(R)CN]^-$ , *anti*-coordination between the catalyst and the allylic substrate leads to a highly thermodynamically stable complex  $intF-R$  ( $\Delta G_{DCM} = -2.8$  kcal/mol) and endergonic  $intF-S$  ( $\Delta G_{DCM} = +3.0$  kcal/mol) (Figure 4). Similar to catalyst  $[LCu(R)Br]^-$ ,  $S_N2'$  through  $TSF-R$  ( $\Delta G_{DCM}^{\ddagger} = +21.5$  kcal/mol relative to  $intF-R$ ) generates  $(R)$ -3a, which is energetically more favorable than through  $TSF-S$  ( $\Delta G_{DCM}^{\ddagger} = +24.4$  kcal/mol relative to  $intF-R$ ) to give  $(S)$ -3a. The activation free energy difference ( $\Delta\Delta G_{DCM}^{\ddagger}$ ) for  $[LCu(R)CN]^-$  is 2.9 kcal/mol in favor of  $(R)$ -3a. Critically, the stable  $intF-R$  would aid in pre-discriminating the *R*- or *S*- pathways from the start and drives the racemization process towards  $(R)$ -1a.<sup>33</sup> This would also rationalize why experimentally,  $CuCN$  performs better than  $CuBr$  (Table 1). In essence, our computational modeling predicted that both the catalysts perform in a highly stereo-discriminatory manner to generate the  $(R)$ -3a product consistent with our experimental

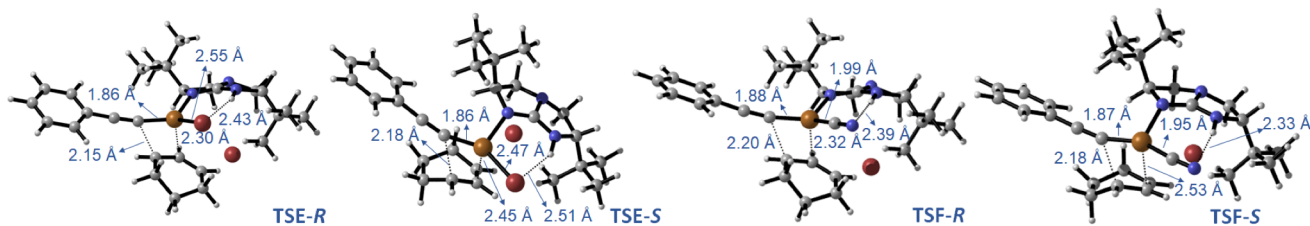
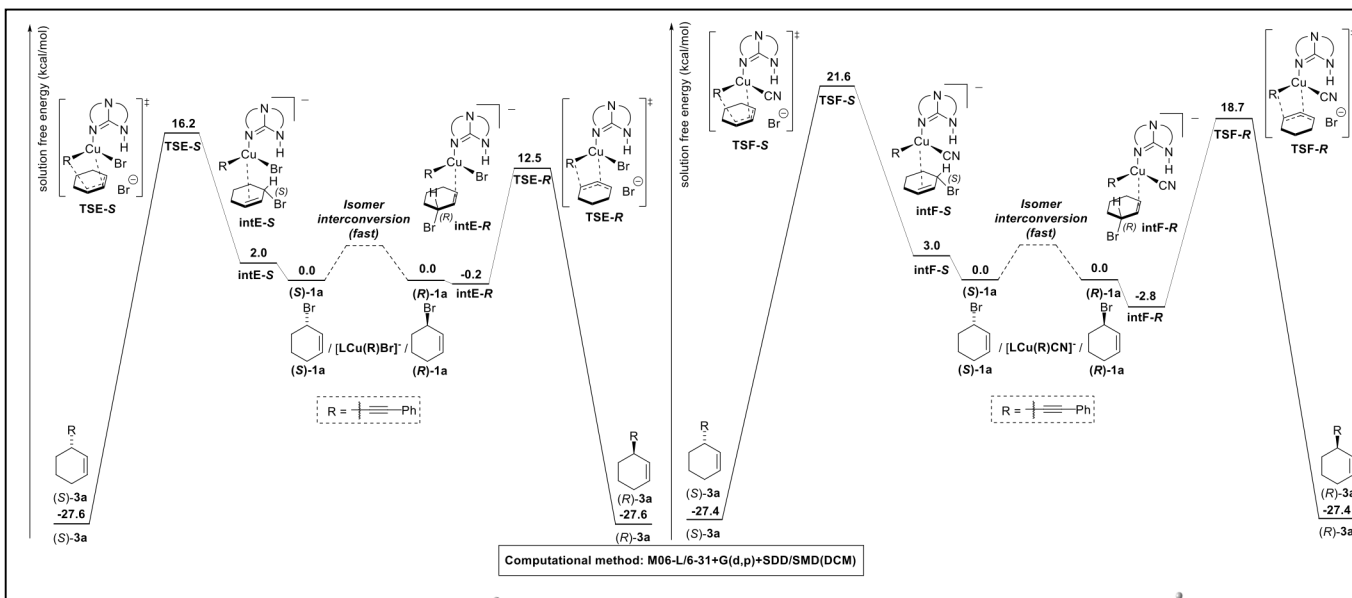


**Figure 4. Mechanistic Free Energy Profiles for  $S_N2'$  Nucleophilic Substitution Pathway with  $[LCu(R)X]^-$ .** Top: Bromide (left) and cyanide (right) cuprate catalytic species undergo  $S_N2'$  nucleophilic substitution in an antarafacial (*anti*-) manner, leading to the formation of *R*- and *S*-enantiomer products. Relative solution free energies, in kcal/mol, are shown. ( $R$  = phenyl alkynide,  $L$  = chiral guanidine ligand) Bottom: Optimized transition state structures  $TSE-R$ ,  $TSE-S$ ,  $TSF-R$  and  $TSF-S$  with key bond distances. Atoms are color-coded gray, brown, maroon, blue and white to represent C, Cu, Br, N and H respectively.

observations.

## CONCLUSIONS

A simple and mild methodology has been developed for enantioselective alkynylation of racemic bromides under biphasic condition. This approach employs functionalized terminal alkynes as pro-nucleophiles and provides 6- and 7-membered cyclic 1,4-enynes with high yields and excellent enantioselectivities. Cold-spray ionization mass spectrometry (CSI-MS) and X-ray crystallography were used to identify catalytic intermediates, which include guanidinium cuprate ion pairs and a copper-alkynide complex. A linear correlation between the enantiopurity of the catalyst and reaction product indicates the presence of a copper complex bearing a single guanidine ligand at the enantio-determining step. Further experimental and computational studies supported that racemic allylic bromides undergo copper-assisted racemization and complexation with  $[\text{LCu}(\text{R})\text{Br}]^-/[\text{LCu}(\text{R})\text{CN}]^-$  in a highly stereo-selective manner, driven either by kinetics, thermodynamics or a combination of both factors to afford the major enantiomer in high yield and optical purity. We are currently investigating (guanidine)copper complex-catalyzed  $\text{C}_{\text{sp}^3}\text{-C}_{\text{sp}^2}$  and  $\text{C}_{\text{sp}^3}\text{-C}_{\text{sp}^3}$  couplings with racemic starting materials.

## ASSOCIATED CONTENT

### Supporting Information

Experimental procedures and compound characterization data. This material is available free of charge via the internet at <http://pubs.acs.org>.

## AUTHOR INFORMATION

### Corresponding Author

[choonhong@ntu.edu.sg](mailto:choonhong@ntu.edu.sg)  
[richmond\\_lee@sutd.edu.sg](mailto:richmond_lee@sutd.edu.sg)

### Funding Sources

We are grateful to the Nanyang Technological University (M401663) and Singapore University of Technology and Design for financial support. We acknowledge National Supercomputing Centre (Singapore) and SUTD HPC for computational resources.

### Notes

The authors declare no competing financial interest.

## ABBREVIATIONS

BG, bisguanidinium; CG, cyclicguanidinium; CSI-MS, Cold-spray ionization mass spectrometry; DET, direct enantio-convergent transformation; DFT, density functional theory; DKR, dynamic kinetic resolution; DYKAT, dynamic kinetic asymmetric transformation; PN, pentanidinium; TS, transition state.

## REFERENCES

- a) Trost, B. M.; Van Vranken, D. L. *Chem. Rev.* **1996**, *96*, 395; b) Cherney, A. H.; Kadunce, N. T.; Reisman, S. E. *Chem. Rev.* **2015**, *115*, 9587.
- The conventional definition is cited here. Depending on substrate and metal, the scope of soft nucleophiles can be expanded to pro-nucleophiles with  $\text{pK}_a$  32.2, see examples: a) Sha, S.-C.; Zhang, J.; Carroll, P. J.; Walsh, P. J. *J. Am. Chem. Soc.* **2013**, *135*, 17602; b) Misale, A.; Niyomchon, S.; Luparia, M.; Maulide, N. *Angew. Chem. Int. Ed.* **2014**, *53*, 7068.
- a) Trost, B. M.; Bunt, R. C. *J. Am. Chem. Soc.* **1994**, *116*, 4089; b) Huerta, F.F.; Minidis, A.B.E.; Bäckvall, J.-E. *Chem. Soc. Rev.* **2010**, *30*, 321; c) Trost, B. M. *Tetrahedron* **2015**, *71*, 5708; d) Bhat, V.; Welin, E. R.; Guo, X.; Stoltz, B. M. *Chem. Rev.* **2017**, *117*, 4528.
- For review of Cu-catalyzed AAAs through  $\text{S}_{\text{N}}2'$  pathway: a) Harutyunyan, S. R.; den Hartog, T.; Geurts, K.; Minnaard, A. J.; Feringa, B. L. *Chem. Rev.* **2008**, *108*, 2824; b) Alexakis, A.; Backvall, J. E.; Krause, N.; Pàmies, O.; Diéguez, M. *Chem. Rev.* **2008**, *108*, 2796; c) Alexakis, A.; Norbert, K.; Simon, W. eds. *Copper-catalyzed asymmetric synthesis.*; Chapter 4, John Wiley & Sons, **2013**. For pioneering works in this area, see: with Grignard reagent, d) van Klaveren, M.; Persson, E. S.; del Villar, A.; Grove, D. M.; Bäckvall, J. E.; van Koten, G. *Tetrahedron Letters*, **1995**, *36*, 3059; e) Tissot-Croset, K.; Polet, D.; Alexakis, A. *Angew. Chem. Int. Ed.* **2004**, *43*, 2426; f) Geurts, K.; Fletcher, S. P.; Feringa, B. L. *J. Am. Chem. Soc.* **2006**, *128*, 15572; g) Selim, K. B.; Matsumoto, Y.; Yamada, K. I.; Tomioka, K. *Angew. Chem. Int. Ed.* **2009**, *48*, 8733; with organozinc reagent, h) Dübner, F.; Knochel, P. *Angew. Chem. Int. Ed.* **1999**, *38*, 379; i) Kacprzynski, M. A.; Hoveyda, A. H. *J. Am. Chem. Soc.* **2004**, *126*, 10676; j) van Veldhuizen, J. J.; Campbell, J. E.; Giudici, R. E.; Hoveyda, A. H. *J. Am. Chem. Soc.* **2005**, *127*, 6877; with organoaluminium reagent, k) Lee, Y.; Akiyama, K.; Gillingham, D. G.; Brown, M. K.; Hoveyda, A. H. *J. Am. Chem. Soc.* **2008**, *130*, 446; with organolithium reagent, l) Pérez, M.; Fañanás-Mastral, M.; Bos, P. H.; Rudolph, A.; Harutyunyan, S. R.; Feringa, B. L. *Nat. Chem.* **2011**, *3*, 377; with organoboranes, m) Shintani, R.; Takatsu, K.; Takeda, M.; Hayashi, T. *Angew. Chem. Int. Ed.* **2011**, *50*, 8656; n) Jung, B.; Hoveyda, A. H. *J. Am. Chem. Soc.* **2012**, *134*, 1490.
- Cu-catalyzed AAAs with racemic starting materials: a) Langlois, J. B.; Alexakis, A. *Chem. Commun.* **2009**, 3868; b) Langlois, J. B.; Alexakis, A. *Adv. Synth. Catal.* **2010**, *352*, 447; c) Langlois, J. B.; Alexakis, A. *Angew. Chem. Int. Ed.* **2011**, *50*, 1877; d) Langlois, J. B.; Emery, D.; Mareda, J.; Alexakis, A. *Chem. Sci.* **2012**, *3*, 1062; e) You, H.; Rideau, E.; Sidera, M.; Fletcher, S. P. *Nature* **2015**, *517*, 351; f) Rideau, E.; Fletcher, S. P. *Beilstein J. Org. Chem.* **2015**, *11*, 2435; g) Sidera, M.; Fletcher, S. P.; *Chem. Commun.* **2015**, *51*, 5044; h) Rideau, E.; You, H.; Sidera, M.; Claridge, T. D.; Fletcher, S. P. *J. Am. Chem. Soc.* **2017**, *139*, 5614; i) Schäfer, P.; Sidera, M.; Palacin, T.; Fletcher, S. P. *Chem Commun.* **2017**, *53*, 12499; j) Fañanás-Mastral, M.; Feringa, B. L. *J. Am. Chem. Soc.* **2010**, *132*, 13152.
- a) Li, H.; Alexakis, A. *Angew. Chem. Int. Ed.* **2012**, *51*, 1055; b) Makida, Y.; Takayama, Y.; Ohmiya, H.; Sawamura, M. *Angew. Chem. Int. Ed.* **2013**, *52*, 5350.
- a) Dabrowski, J. W.; Gao, F.; Hoveyda, A. H. *J. Am. Chem. Soc.* **2011**, *133*, 4778; b) Harada, A.; Makida, Y.; Sato, T.; Ohmiya, H.; Sawamura, M. *J. Am. Chem. Soc.* **2014**, *136*, 13932; c) Hamilton, J. Y.; Sarlah, D.; Carreira, E. M. *Angew. Chem. Int. Ed.* **2013**, *52*, 7532.
- a) Coles, M. P.; Hitchcock, P. B. *Polyhedron* **2001**, *20*, 3027; b) Oakley, S. H.; Coles, M. P.; Hitchcock, P. B. *Inorg. Chem.* **2004**, *43*, 5168; c) Coles, M. P. *Dalton Trans.* **2006**, 985; d) Coles, M. P. *Chem. Commun.* **2009**, 3659.
- Chiral guanidine ligand in transition metal catalysis: a) Zhu, Y.; Liu, X.; Dong, S.; Zhou, Y.; Li, W.; Lin, L.; Feng, X. *Angew. Chem. Int. Ed.* **2014**, *53*, 1636; b) Tang, Y.; Chen, Q.; Liu, X.; Wang, G.; Lin, L.; Feng, X. *Angew. Chem. Int. Ed.* **2015**, *54*, 9512; c) Chen, Q.; Tang, Y.; Huang, T.; Liu, X.; Lin, L.; Feng, X. *Angew. Chem. Int. Ed.* **2016**, *55*, 5286; d) Kim, B.; Chinn, A. J.; Fandrick, D. R.; Senanayake, C. H.; Singer, R. A.; Miller, S. J. *J. Am. Chem. Soc.* **2016**, *138*, 7939; e) Chinn, A. J.; Kim, B.; Kwon, Y.; Miller, S. J. *J. Am. Chem. Soc.* **2017**, *139*, 18107.
- a) Wang, C.; Zong, L.; Tan, C. H. *J. Am. Chem. Soc.* **2015**, *137*, 10677; b) Ye, X.; Moeljadi, A. M. P.; Chin, K. F.; Hirao, H.; Zong, L.; Tan, C. H. *Angew. Chem. Int. Ed.* **2016**, *55*, 7101; c) Teng, B.; Chen, W.; Dong, S.; Kee, C. W.; Gandamana, D. A.; Zong, L.; Tan, C. H. *J. Am. Chem. Soc.* **2016**, *138*, 9935; d) Zong, L.; Wang, C.; Moeljadi, A. M. P.; Ye, X.; Ganguly, R.; Li,

- Y.; Hirao, H.; Tan, C.-H. *Nat Commun.* **2016**, *7*, 13455; e) Zong, L.; Tan, C. H. *Acc. Chem. Res.* **2017**, *50*, 842.
- (11) a) Jeffery, T. *Tetrahedron Letters* **1989**, *30*, 2225; b) Grushin, V. V.; Alper, H. *J. Org. Chem.* **1992**, *57*, 2188.
- (12) a) Ma, T.; Fu, X.; Kee, C. W.; Zong, L.; Pan, Y.; Huang, K. W.; Tan, C. H. *J. Am. Chem. Soc.* **2011**, *133*, 2828; b) Yang, Y.; Moinodene, F.; Chin, W.; Ma, T.; Jiang, Z.; Tan, C. H. *Org. Lett.* **2012**, *14*, 4762; c) Zong, L.; Ban, X.; Kee, C. W.; Tan, C. H. *Angew. Chem. Int. Ed.* **2014**, *53*, 11849; d) Zong, L.; Du, S.; Chin, K. F.; Wang, C.; Tan, C. H. *Angew. Chem. Int. Ed.* **2015**, *54*, 9390.
- (13) a) Leow, D.; Tan, C. H. *Synlett* **2010**, *11*, 1589; b) Wang, C.; Goh, C. M. T.; Xiao, S.; Ye, W.; Tan, C. H. *J. Synth. Org. Chem. Jpn.* **2013**, *71*, 1145; c) Chen, W.; Yang, W.; Yan, L.; Tan, C. H.; Jiang, Z. *Chem. Commun.* **2013**, *49*, 9854.
- (14) Sidera, M.; Fletcher, S. P. *Nature Chemistry*, **2015**, *7*, 935.
- (15) a) Liu, H.; Leow, D.; Huang, K.-W.; Tan, C.-H. *J. Am. Chem. Soc.* **2009**, *131*, 7212; b) Dabrowski, J. A.; Haeffner, F.; Hoveyda, A. H. *Angew. Chem. Int. Ed.* **2013**, *52*, 7694.
- (16) Yum, E. K.; Larock, R. C. *J. Am. Chem. Soc.* **1991**, *113*, 6690.
- (17) Meldal, M.; Tornøe, C. W. *Chem. Rev.* **2008**, *108*, 2952.
- (18) a) Maligres, P. E.; Krska, S. W.; Dormer, P. G. *J. Org. Chem.* **2012**, *77*, 7646; b) Benkovics, T.; Du, J.; Guzei, I. A.; Yoon, T. P. *J. Org. Chem.* **2009**, *74*, 5545.
- (19) a) Woodward, S. *Chem. Soc. Rev.* **2000**, *29*, 393; b) Yoshikai, N.; Nakamura, E. *Chem. Rev.* **2012**, *112*, 2339.
- (20) Cold-spray ionization mass spectrometry is a variant of ESI-MS operating at low temperature to characterize thermally unstable or sensitive organic complex: a) Yamaguchi, K. *J. Mass Spectrom.* **2003**, *38*, 473; b) Tsybizova, A.; Roithova, J. *Mass Spectrom. Rev.* **2016**, *35*, 85.
- (21) a) Lang, H.; Jakob, A.; Milde, B. *Organometallics*, **2012**, *31*, 7661; b) Worrell, B. T.; Malik, J. A.; Fokin, V. V. *Science*, **2013**, *340*, 457.
- (22) a) Wynberg, H.; Feringa, B.; *Tetrahedron* **1976**, *32*, 2831; b) Kalek, M.; Fu, G. C. *J. Am. Chem. Soc.* **2017**, *139*, 4225.
- (23) a) Bissember, A. C.; Lundgren, R. J.; Creutz, S. E.; Peters, J. C.; Fu, G. C. *Angew. Chem. Int. Ed.* **2013**, *52*, 5129; b) Kainz, Q. M.; Matier, C. D.; Bartoszewicz, A.; Zultanski, S. L.; Peters, J. C.; Fu, G. C. *Science* **2016**, *351*, 681; c) Fu, G. C. *ACS Cent. Sci.* **2017**, *3*, 692.
- (24) a) Ito, H.; Kunii, S.; Sawamura, M. *Nat. Chem.* **2010**, *2*, 972; b) Roggen, M.; Carreira, E. M. *Angew. Chem. Int. Ed.* **2016**, *51*, 8652.
- (25) a) Goering, H. L.; Nevitt, T. D.; Silversmith, E. F. *J. Am. Chem. Soc.*, **1955**, *77*, 4042; b) Lesnini, D. G.; Buckley, P. D.; Noyes, R. M. *J. Am. Chem. Soc.* **1968**, *90*, 668; c) Streitwieser, A.; Jayasree, E. G.; Hasanayn, F.; Leung, S. H. *J. Org. Chem.* **2008**, *73*, 9426.
- (26) Li, C.; Zhang, Y.; Sun, Q.; Gu, T.; Peng, H.; Tang, W. *J. Am. Chem. Soc.* **2016**, *138*, 10774.
- (27) Trost, B. M.; Verhoeven, T. R., *J. Org. Chem.* **1976**, *41*, 3215.
- (28) a) Matsushita, H.; Negishi, E. *J. Chem. Soc. Chem. Commun.* **1982**, 160; b) Corey, E. J.; Boaz, N. W. *Tet. Letters* **1984**, *25*, 3063.
- (29) a) Sha, S.-C.; Jiang, H.; Mao, J.; Bellomo, A.; Jeong, S. A.; Walsh, P. J. *Angew. Chem. Int. Ed.* **2016**, *55*, 1070; b) Mao, J.; Zhang, J.; Jiang, H.; Bellomo, A.; Zhang, M.; Gao, Z.; Dreher, S. D.; Walsh, P. J. *Angew. Chem. Int. Ed.* **2016**, *55*, 2526.
- (30) a) Yamanaka, M.; Kato, S.; Nakamura, E. *J. Am. Chem. Soc.* **2004**, *126*, 6287; b) Casitas, A.; Ribas, X. *Chem. Sci.* **2013**, *4*, 2301; c) Yasuda, Y.; Ohmiya, H.; Sawamura, M. *Angew. Chem. Int. Ed.* **2016**, *55*, 10816.
- (31) a) Bartholomew, E. R.; Bertz, S. H.; Cope, S.; Murphy, M.; Ogle, C. A. *J. Am. Chem. Soc.* **2008**, *130*, 11244. b) Yoshikai, N.; Zhang, S. L.; Nakamura, E. *J. Am. Chem. Soc.* **2008**, *130*, 12862.
- (32) a) Goering, H. L.; Kantner, S. S.; Tseng, C. C. *J. Org. Chem.* **1983**, *48*, 715; b) Ruan, J.; Iggo, J. A.; Berry, N. G.; Xiao, J. *J. Am. Chem. Soc.* **2010**, *132*, 16689.
- (33) a) Zhu, B.; Lee, R.; Li, J.; Ye, X.; Hong, S. N.; Qiu, S.; Coote, M. L.; Jiang, Z. *Angew. Chem. Int. Ed.* **2016**, *55*, 1299; b) Zhu, B.; Qiu, S.; Li, J.; Coote, M. L.; Lee, R.; Jiang, Z. *Chem. Sci.* **2016**, *7*, 6060.

For Table of Contents Only

